Detecting Faint Secondary Stars with Shaped Aperture Masks

Donald Loveland[1], Edward Foley[1], Russell Genet[1], Neil Zimmerman[2],
David Rowe[3], Richard Harshaw[4], and Jimmy Ray[5]

1. California Polytechnic University, San Luis Obispo, California
2. Space Telescope Science Institute, Maryland
3. PlaneWave Instruments, Rancho Dominguez, California
4. Brilliant Sky Observatory, Cave Creek, Arizona
5. Arizona Desert Sonoran Observatory, Glendale, Arizona

Abstract Two shaped aperture masks were evaluated to test for useful ranges when examining double stars with large differential magnitudes and separation. Through observations of multiple double stars, the Gaussian Donut mask showed no conclusive evidence that it was more successful than an unmasked telescope. Due to the detection ability of speckle interferometry alone, and a relatively large diffraction pattern from the mask, the Gaussian Donut mask was unable to make a significant difference. Comparatively, the Bow Tie mask showed promise with a small diffraction pattern allowing for close inner working angles of near 1″. Given the current boundaries, further investigation of the mask's abilities will allow for better detection and the resolving of close double stars.

Introduction

Diffraction

Diffraction occurs when an opening is placed in the path of a beam of light causing the light to bend around the edge. Smaller openings cause the light to bend extensively, while a larger opening will cause a much less noticeable phenomenon. Famous experiments such as the double and single slit experiment exhibit this, as well as demonstrating the wave-particle duality principle of light. The light bends around the edges as waves, which allows for destructive and constructive interference. This causes an overall diffraction pattern of bright and dark regions where there is constructive interference and destructive interference respectively. Figure 1 shows the diffracted waves and how they come to fruition on the screen. There are clear bands created where the waves end with constructive interference. With this in mind, other diffraction patterns can be created depending on the shape of the obstruction and how the light is diffracted. Figure 1 demonstrates the famous Airy Disk pattern which is created by a circular opening. The light diffracts in such a way to create concentric rings around the central fringe outward. The rings demonstrate an area of constructive interference of the light going through the circular opening.

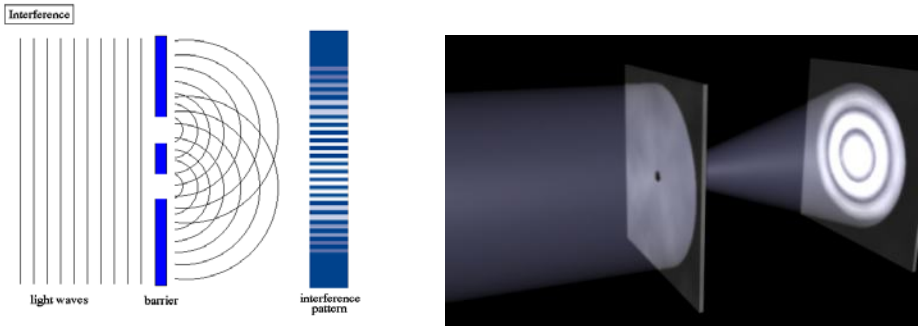

Figure 1. The left image shows the double slit experiment. The right image shows the circular aperture diffraction pattern.

The diffraction from the circular opening works similar to how a telescope diffracts light from a star. Fraunhofer diffraction simplifies diffraction by assuming a star is far enough away to treat it as an infinitely far away object. With this condition, the telescope aperture can be treated as a single point circular opening, causing the same diffraction pattern. Figure 2 shows this diffraction on a simulated single star with an Airy Disk pattern around it.

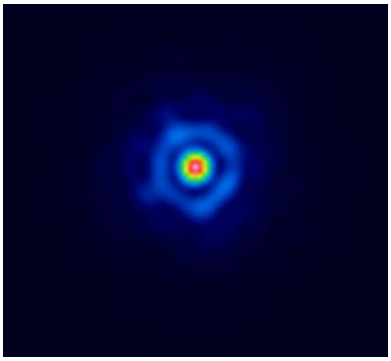

Figure 2. Simulated Star with Airy Pattern.

Importance for Binary Stars

The Airy Disk pattern occurs with any star that is observed through a circular aperture, which is the phenomenon that occurs through all telescopes. As seen in Figure 3, this feature can be very prominent when observing a double star, as the ring can potentially block a secondary star.

The primary focus of the project was to promote the discovery of binary star systems that have large differential apparent magnitudes as well as close separations. These normally would be heavily disrupted by the Airy Disk pattern. With a large differential apparent magnitude, the brighter star's diffraction pattern will easily engulf the much fainter star. In addition to this, having the stars in close proximity causes the secondary star to be within the range of the diffraction. Figure 3 shows a simulation of a binary star system with about 1″ of separation and only two differential orders of magnitude between them. This shows the damaging effects of a bright main star with close separation to its companion star in how difficult it is to resolve them.

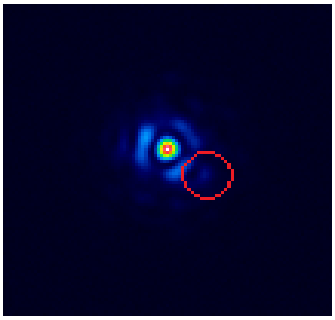

Figure 3. A Simulated Binary Star System with 1" separation and two differential orders of magnitude in Atmospheric Seeing Distortion simulator. The red circle demonstrates the placement of the secondary star.

Why do these specific binary stars matter?

Spectral classification assigns a letter based on the surface temperature of a star. The scale goes through the letters O, B, A, F, G, K, and M, where O stars are relatively hot and M stars are relatively cool. With this temperature gradient in mind, and knowing the Stefan-Boltzmann law $E = \sigma T^4$, it becomes evident that

cooler stars will have a much lower energy output (Peterson and Ryden 2010). This energy output directly correlates to the luminosity of the star. In a binary star system with a hotter star and a cool M star, the M star will be easily drowned out based on luminosity. This does not take into account atmospheric distortion and the Airy Disk diffraction that exacerbates the situation. M class stars are difficult to find, leading to an underrepresentation on the HR diagram critical in pinpointing the composition of our universe.

Similar to the spectral classification, being able to determine if the system is a binary or optical double is crucial. One way to do this is to determine the motion of the star; if they are gravitationally bound they will rotate around one another, and if not they will simply move apart. With widely separated stars, the movements will be difficult to detect because the periods can move up to hundreds of years or longer. Knowing Keplar's Law of Periods, $P^2 = a^3$, it becomes evident the period grows very quickly as the separation increases (Peterson and Ryden 2010). Being able to find very close binary and double stars makes the process much easier, as the period will be much shorter and actually noticeable as compared to wider binaries.

Origin of Aperture Masks

The idea for diffraction masks started out as a technique to discover exoplanets and is now being applied to double star research. Exoplanets will behave just as the double star systems being observed, as it will be revolving around a much brighter stellar body. Both issues found in binary star discovery lie in the nature of exoplanet research. For the large delta magnitude problem, this will be heavily magnified because the exoplanets will not be emitting any sort of light. The only light that will be seen will be what is reflected by it. This can cause these planets to become quite dim in relation to a secondary star component of a binary system, making them even more difficult to find.

As for the second problem, the habitable zone is an area where exoplanets will be most useful as that is where they could harbor life. This distance ranges anywhere from a quarter of an astronomical unit to 15 astronomical units, causing the resulting small separation to also be a difficult factor. Aperture masks for this problem would need to allow for enough light gathering power while also allowing for smaller inner working angles. These two combat one another due to larger obstructions causing smaller diffraction patterns. Conversely, as the mask is made larger, light gathering power is forfeited, causing a tradeoff.

For the moment, the transit method is used by NASA with great accuracy, but aperture masks would be well suited to allow for direct observing of these exoplanets. Using the transit method, an actual transit must occur, limiting when data can be taken. Furthermore, the exoplanet must be edge-on with the star, further limiting the ability to view. The aperture mask can fix this problem, allowing for the ability to view the planet at any position and allowing for the ability to find new exoplanets not previously discovered. Aperture masks can aid in the determination of the location of an exoplanet versus only using the transit method, allowing for more information to be discovered and logged.

Designing and Creating the Diffraction Masks

In determining whether a diffraction mask will be useful, the first step involves creating a simulated version of the mask in MATLAB. MATLAB is a computation environment capable of handling development as well as analysis of data. More importantly, MATLAB excels in handling matrix computation, which is relied on in mask design. A matrix the size of the mask is created and assigned either zeroes or ones. The numbers represent the brightness of the pixel it is assigned to. The number one tells MATLAB to turn the pixel white, while a zero tells it to turn the pixel black. The aperture mask itself is comprised of all the black pixels.

Taking the Fourier transform of this decomposes the mask's frequency into the most basic sinusoidal waves it's comprised of, which demonstrates where the diffraction will occur. When creating the original outline for the mask, there are two basic principles that need to be followed in the design. First, as the size of the obstruction gets bigger, there are more sinusoidal waves that can fit in the original frequency, causing a stronger, more inward diffraction pattern. Secondly, as the obstruction gets smaller, fewer waves can fit, causing a weaker, more outward diffraction pattern.

Once a mask has been proposed and determined to be efficient in terms of allowing for a close inner working angle and large discovery zones, it can be physically created. Sturdy but light materials such as acrylic and foam core have worked well as aperture masks. Next, the material needs to be laser cut using the outline from the MATLAB processes. It is important to be aware of widths and sizes to obtain a clean cut. Once cut, the mask is best sprayed with a dull black color in order to not interact with any light waves.

Diffraction Masks

With the airy pattern disrupting the viewing of a secondary star, it becomes important to attempt to push this light in a different direction with the intent to form "discovery zones." These zones are where the secondary star can be observed. These discovery zones are places of destructive interference of light from the primary star due to the wave nature of light that allow for easier viewing. Understanding that the telescope aperture acts no different than pinhole diffraction, the shape of the aperture can be changed to achieve different forms of diffraction patterns.

Changing the aperture can be done by using diffraction masks which are disks that go in front of the telescope. The masks effectively change how the light will bend. The first mask proposed was the Gaussian Donut mask, designed by Ed Foley, which can be seen in Figure 4. This design was based off of a Gaussian curve mask developed by Kasdin and his group (Kasdin et al. 2003). On the left of Figure 4 is the actual shape of the mask and what will be obstructing the front of the telescope. On the right of the image is the theoretical diffraction pattern that occurs when the telescope is obstructed by the mask. The darker triangular areas on the left and right side of the pattern are the areas where the secondary star would want to be placed, as that is where the light is destructively interfering.

The primary goals of the masks are to achieve a strong contrast ratio between the darker and lighter regions, and achieve a small working angle to resolve closely separated binary stars. The working angle is where the secondary star can be placed to allow us to see it. The darker regions will allow the ability to resolve fainter stars, and the smaller working angle will allow for resolution of closer stars. The Gaussian mask itself is theorized to best be used at wider working angles, 4" to 7" for the Celestron C-11 that is being used for this project.

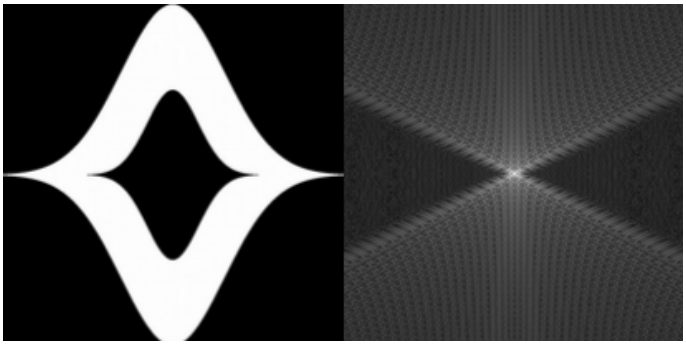

Figure 4. Gaussian Donut Mask shape with diffraction simulation to the right.

The second mask evaluated was the Bow Tie mask, which was designed by Neil Zimmerman at Princeton. This mask, seen in Figure 5, does not have as clearly defined discovery zones as the Gaussian mask, but instead gives closer working angles. The brighter area in the center of the diffraction pattern on the right shows where most of the light will be diffracted, while the darker is where the light from the primary will destructively interfere. The inner dark circle is theorized to work at 1″, which is much closer than the Gaussian Donut's 4″ to 7″. On the other hand, the area of discovery is quite small and will be much harder to position.

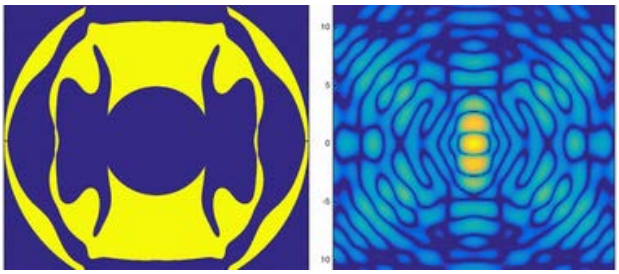

Figure 5. The Bow Tie mask designed by Neil Zimmerman. The mask shape is on the left and the diffraction pattern is on the right.

Equipment

All of the data was taken on the Celestron C-11 Schmidt-Cassegrain telescope at the Orion Observatory. The C-11 optical tube assembly sits on a German equatorial mount with full range of motion. The setup used involved back end instrumentation for easier imaging. The instrumentation revolves around a flip mirror that directs light into a Canon DSLR acquisition camera. Once centered, it can be flipped to an Andor Luca EMCCD for imaging. The set up can be seen in Figure 6. The EMCCD camera used a TeleVue 2.5x Barlow lens on targets above 2″ and was set to 20ms exposures, taking 1000 images to create a data cube. Each image was taken at 128 by 128 pixels. The camera was controlled through a Windows 8 laptop with Andor Solis Imaging software and the data was reduced with Dave Rowe's Plate Solve 3 (Rowe & Genet 2015). The masks used were cut out of acrylic and placed on the front end of the telescope; one of the masks, the "Gaussian Donut," can be seen on the front end of the C-11 in Figure 6.

Figure 6. The left image shows the back end imaging components, the right image shows the Gaussian Donut mask on the C-11 telescope.

Data

Images taken through the Andor Luca EMCCD camera were taken as .sif files and translated into fits cubes. The fits cubes are then able to be speckle reduced in Plate Solve 3. When acquiring the actual data, three to five sets of data were taken for each binary pair. The first set of data was images with no aperture mask in front of the telescope. This was done to provide a control to compare further images. If the stars were greater than 6″ in separation, only the Gaussian Donut mask was used to take data. If the stars were under 4″ only the Bow Tie mask will be used. If the star is between 4″ and 6″, both masks will be used due an ambiguity in masks' limits. When using a mask, a data set was taken from a neutral position in 30° intervals up to 90° position to find the best spot for the closest inner working angle. The masks have symmetrical diffraction patterns; therefore going through the whole rotation will not be necessary, although multiple spots are needed due to the small angle of the discovery zones.

A list was compiled from the WDS catalog of 119,400 stars to find appropriate targets for imaging. Due to being in the Northern Hemisphere, any stars with negative declination were taken out, leaving 70,696 stars. Next, stars with separations between 1″ and 15″ were chosen to give a wide range of targets. Anything above 15″ was unnecessary and anything below 1 would be under the theoretical limit of the telescope itself. This constraint dropped the list of stars to 35,378. In addition, any secondary star lower than 12th magnitude was taken out due to the limit of the EMCCD camera coupled with the telescope's aperture. Anything that faint would be undetectable and thus unnecessary, bringing the star list down to 14,105. Filtering the primary stars to only 7th magnitude and brighter to achieve easy finding pushed the list much farther down to 601 candidates. Lastly, an RA filter of 13hours to 20hours left 163 final candidates that filled all of the requirements.

The data section below has two components, discussing each mask on its own. The first section discusses the Gaussian Donut mask, exploring limits and usefulness. The second section discusses the Bow Tie mask, investigating the same information. The left image is the double star without a mask, and on the right with a mask.

Star List

Star Name	Separation	Mag. 1	Mag. 2	Delta Magnitude	Mask Used
BU 287	7.2	2.96	12	9.04	GD
STF 2140	4.7	3.48	5.4	1.92	GD/BT
STF 2579	2.5	2.89	6.27	3.38	BT
BU 627	1.8	4.84	8.45	3.61	BT

Table 1. Star list that was used to obtain data.

Gaussian Donut Mask

BU 287 was imaged without a deconvolution star. The secondary component of the binary system was near the limit of the equipment's detecting ability, which was around 12th magnitude, and difficult to get desirable results. The primary star is 2.9th magnitude, causing the secondary star to be drowned out and hard to resolve. The image on the left in Figure 7 with no mask demonstrates detection of the faint secondary star. Although difficult to see, it can be seen near the top right of the image. The image on the right in Figure 7 shows the double star with the Gaussian Donut mask, where the secondary star is a faint smudge. Placing an aperture mask on the telescope ultimately blocks portions where light can be gathered, potentially causing a star at the limit of the unmasked set up undetectable.

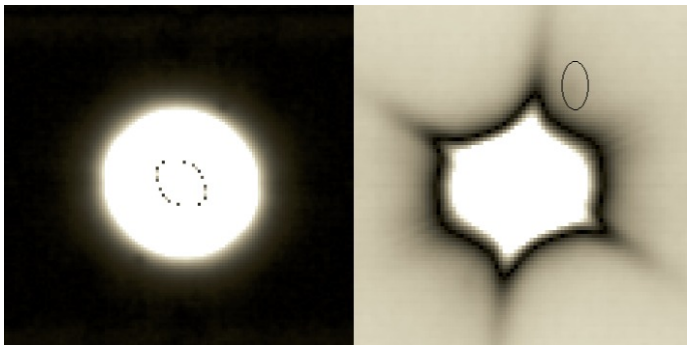

Figure 7. Images of binary star BU 287. The left shows the unmasked image while the right shows the masked image.

STF 2140 was imaged without a deconvolution star. The secondary star was only two orders of magnitude lower than the primary star at 5.4th magnitude, making it very bright. The main focus of this image was to determine an inner working angle for the mask. With no mask, the airy null pattern doesn't seem to be as clear. This could be an overexposure issue that is weakened once a mask is able to block out light. As for working angles, the star still has some room to move inward. This demonstrates the spot necessary to achieve the closest inner working angle, in the smallest triangular regions.

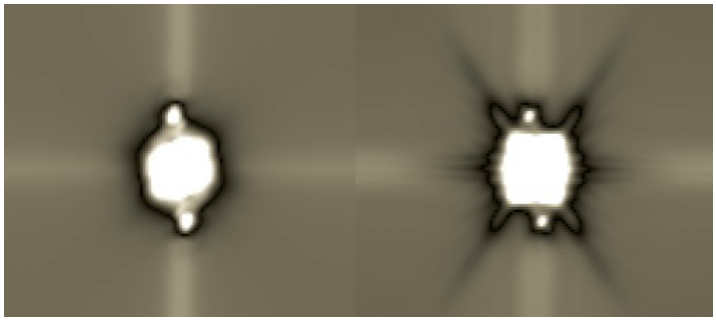

Figure 8. Images of binary star STF 2140. Main focus is on the large diffraction spikes from the aperture mask.

Bow Tie Mask

STF 2140 had a deconvolution star used on both images. Considering the same magnitudes, this image was primarily used to test inner working angles. The left image in Figure 9 shows the pair with no mask, and the right image shows the pair with the mask. The secondary star has a clear airy disk pattern with clear room to continue to move in further. When using the astrometry tool in Plate Solve 3 the inner working angle shows to be approximately 1.8″, which can be closer under better conditions.

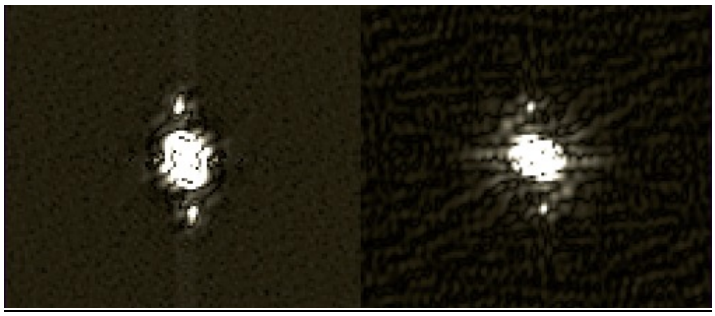

Figure 9. Images of binary star STF 2140. The secondary component of the system is much clearer and circular in the masked image in comparison to the unmasked image.

STF 2579 used a deconvolution star for both of the images due to what was found in the STT 328 images. By being separated by 2.5″ the binary star system falls under the 4″ limit where a deconvolution would not be required. The bright primary star of 2.9th magnitude and the secondary star of 6.7th magnitude don't produce a large differential magnitude, but it works well in determining an inner working angle for the mask. In the image with no mask, it is clear the diffraction pattern of the primary star is beginning to interfere with the detection of the secondary star. The airy null pattern is neither complete nor is it as dark in comparison to the image with a mask. The image with the mask clearly demonstrates the Bow Tie mask's theoretical diffraction pattern, and when analyzed with the astrometry tool, it shows an approximate 1.5″.

Figure 10. Images of binary star STF 2579. There is clear demonstration of the Bow Tie diffraction pattern with a much more defined outline of the secondary component.

BU 627 used a deconvolution star for both of the images. With the primary component of the system being 4.8th magnitude and the secondary component being 8.5th magnitude, the main purpose of this image was to further refine the inner working angle of the mask. BU 627 is separated by 1.8″ which is clear when compared to STF 2579 and how close the secondary star sits near the primary star. The secondary star also starts to become less noticeable in comparison, due to the drops in magnitude. With the mask, the secondary component has a clear airy null pattern surrounding it, making it much easier to pinpoint. Using the astrometry tool just as in STF 2579, a limit of 1.2″ is shown, which is better than in the previous image.

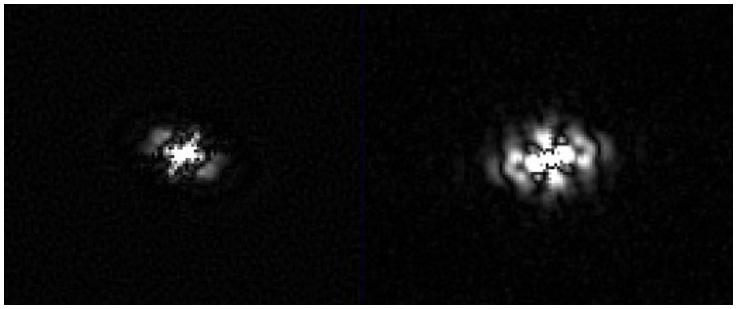

Figure 11. Images of binary star BU 627.

Conclusion

Through the analysis of numerous double stars with both the Gaussian Donut and Bow Tie mask, rough estimates can be made of where they work their best, based on an 11 inch aperture telescope. The Gaussian Donut appears to be useful, but unnecessary due to the independent ability of speckle reduction. The diffraction pattern diffuses out approximately 4″, while speckle reduction is shown to easily reach 2″ and lower. When observing large differential magnitudes, the mask also had difficulty detecting much fainter components. This may have been an issue in the 11 inch aperture, losing light gathering power as the mask obstructed the opening.

The Bow Tie mask showed promising results by demonstrating very close working angles that were able to surpass the ability of speckle reduction without any mask. In STF 2579 and BU 627 the diffraction of the primary component could be seen interfering with the airy null of the secondary component without a mask. With the Bow Tie mask, the diffraction was diffused outward, allowing better contrast inward and thus better detection. With the theoretical discovery zone of the Bow Tie mask residing around 1″, this was able to be further supported with multiple images of the double stars, giving room for continual observations.

References

Kasdin, J., Vanderbei, R., Spergel, D., & M. Littman. 2003. Extrasolar Planet Finding via Optimal Apodized-Pupil and Shaped-Pupil Coronographs. The Astrophysical Journal 582, 1147. http://adsabs.harvard.edu/abs/2003ApJ...582.1147K

Peterson, B. & Ryden, B. 2010. *Foundations of Astrophysics 1st Edition.* Boston, Massachusetts: Addison-Wesley.

Rowe, D. & Genet, R. 2015. User's Guide to PS3 Speckle Interferometry Reduction Program. Journal of Double Star Observations 11, 266.